UCRL-10621

University of California

Ernest O. Lawrence Radiation Laboratory

NEUTRAL-PION PRODUCTION FROM PROTON-PROTON COLLISION AT 735 MEV

DISCLAIMER

Submitted to Phys. Rev.

UCRL-10621

UNIVERSITY OF CALIFORNIA

Lawrence Radiation Laboratory
Berkeley, California

Contract No. W-7405-eng-48

NEUTRAL-PION PRODUCTION FROM PROTON-PROTON COLLISIONS AT 735 MeV

Robert J. Cence, Don L. Lind, Gilbert D. Mead, and Burton J. Moyer

April 15, 1963

Neutral-Pion Production from Proton-Proton Collisions at 735 MeV

Robert J. Cence, Don L. Lind, Gilbert D. Mead, and Burton J. Moyer

Lawrence Radiation Laboratory
University of California
Berkeley, California

April 15, 1963

ABSTRACT

An investigation has been made of the reaction $p + p \rightarrow p + p + \pi^0$ at an incident proton energy of 735 MeV. The external proton beam of the 184-inch synchrocyclotron bombarded a liquid-hydrogen target. Gamma-ray energy spectra were measured at laboratory angles of 6, 32, and 60 deg with respect to the proton beam. Two high-resolution pair spectrometers were used to make these measurements. Computer codes were used to make all necessary corrections to the data and determine the final spectra.

No evidence is found for high-energy gamma rays produced from any source other than neutral-pion decay. The cross section for π^0 production was measured to be 3.46±0.25 mb. By use of the method of least squares, angular and momentum distributions of the neutral pion in the two-proton barycentric system were determined from the photon spectra. The pion angular distribution is given by

$$\frac{d\sigma_{\pi^0}}{d\Omega} = \frac{\sigma_T}{4\pi} [0.834 + 0.099(3\cos^2\theta) + 0.067(5\cos^4\theta)],$$

where θ is the barycentric angle of emission. Pion momentum distributions are given for three angles. The results are shown to give reasonable agreement with the isobar model.

Neutral-Pion Production from Proton-Proton Collisions at 735 MeV*

Robert J. Cence, Don L. Lind, Gilbert D. Mead, and Burton J. Moyer

Lawrence Radiation Laboratory
University of California
Berkeley, California

April 15, 1963

I. INTRODUCTION

The reaction

$$p + p \rightarrow p + p + \pi^0 \qquad (1)$$

possesses certain unique characteristics. Near threshold the cross section for this reaction is severely suppressed.[1,2] At a laboratory energy of 340 MeV the total cross section for (1) is about one-thirtieth of the total cross section for

$$p + n \rightarrow p + n + \pi^0. \qquad (2)$$

This experimental fact is now well understood as being due to the Pauli exclusion principle combined with the fact that the π^0 has odd parity.[1,3,4] The total cross section for reaction (1) is plotted in Fig. 1.

The information on angular distributions is much more limited, primarily because the gamma-ray angular distributions only weakly reflect the neutral-pion angular distributions. One must measure gamma-ray fluxes very accurately to obtain even limited accuracy for π^0 distributions, unless one can measure the energy spectra of the gamma rays as well.

The angular distribution for reaction (1) can be expressed by expanding in even powers of $\cos\theta$; i.e., $d\sigma/d\Omega \propto (1+3b\cos^2\theta + 5c\cos^4\theta + \cdots)$, where θ is the angle of emission in the barycentric system. Odd powers of $\cos\theta$ cannot appear because of the symmetry between the two protons. In the experiments that have

been done so far, terms higher than $\cos^2\theta$ have not been needed to fit the data. Unfortunately, experiments below 440 MeV were not precise enough to make a conclusive determination of even the $\cos^2\theta$ term.[6, 10]

Prokoshkin and Tiapkin find that at 445 MeV, $b \approx 1$; i.e., approximately equal numbers of pions are distributed isotropically and with a $\cos^2\theta$ distribution.[11] At 660 MeV they find that the distribution has become isotropic. In contrast to this, Dunaitsev and Prokoshkin find that the pions are produced isotropically over the entire region from 400 to 660 MeV.[5] The results of York et al. at 397 to 445 MeV are also consistent with isotropic production.[12] The only experiment on hydrogen done with a pair spectrometer finds $b = 0.1 \pm 0.03$ at 660 MeV.[13]

Information on the π^0 energy distribution in reaction (1) is almost nonexistent. One must have accurate gamma-ray spectra at several angles of view to obtain this information, and this has not been available. Baiukov and Tiapkin find that at 660 MeV the most probable π^0 energy is about 0.45 times the maximum available.[13]

The purpose of our experiment was to obtain more detailed information on the π^0 angular and energy distribution in reaction (1) than has been available heretofore. From the Russian work at slightly lower energies it is expected that the angular distribution will be nearly isotropic at 735 MeV incident-proton energy. Furthermore, the isobar model may be expected to play an important role.

II. EXPERIMENTAL METHOD[14]

In this experiment the external proton beam traversed a liquid-hydrogen target in the proton cave of the 184-inch cyclotron. The physical layout used for the 6-deg setup is shown in Fig. 2. The arrangement of the magnets differed only slightly for the other two angles.

The mean energy of the proton beam at the center of the target was 735 MeV. The average intensity was 2×10^{11} protons/sec. Through use of an auxiliary dee, this beam was spilled out evenly over a period of 8 msec, giving a duty cycle of

approximately 50%. It was monitored by means of a secondary-emission chamber similar to that used by Larsen.[15]

The flask of the liquid-hydrogen target was 6-in. thick. The external construction was such that a thin window permitted us to view the gamma rays at any angle between 0 and 90 deg in the laboratory.

Gamma-ray energy spectra were measured by either of two pair spectrometers, both of which used plastic scintillators to count the electrons and positrons. For the energy region 20 to 100 MeV we used a conventional 180-deg spectrometer with six positron and six electron counters. For the energy region 100 to 650 MeV we used a spectrometer which had the unusual geometry shown in Fig. 3. In endeavoring to minimize multiple counts due to electron scattering, this arrangement was found to be distinctly superior to the conventional design in which the counters are arrayed in two straight lines diverging from the converter center.

In both of our spectrometers the light pulses from the scintillators were piped to 6810A photomultipliers via lucite light pipes oriented vertically in long holes drilled through the poles and yoke of the "ORION" H magnet. Details concerning the design and operation of these spectrometers will be published elsewhere.[16]

Between the last sweeping magnet (M_4 in Fig. 2) and the pair spectrometer we placed a counter using a 0.020-in.-thick plastic scintillator. It functioned in anticoincidence with the spectrometer counters in order to eliminate events due to charged particles that had escaped sweeping magnets M_3 and M_4. Using this counter we were able to increase the converter in-out ratio by about a factor of two.

The electronic system used to determine electron-positron coincidences is shown in a simplified block diagram in Fig. 4. The eight signals from each side (six in the case of the 180-deg spectrometer) were first added together. The summed signals were put into a Wenzel-type coincidence circuit[17] to determine two-fold coincidences along with the signal from the anticoincidence counter mentioned above.

The resolving time of this circuit was approximately 10 nsec (full width at half maximum). The fast output triggered a gate, which in turn informed the binary coder that an event had taken place. The binary coder then recorded the signals from the particular counters which had produced a signal over the past 20 nsec. Pulses in binary code were then transmitted to a core storage matrix. On command, the core storage unit read out the number of counts in each channel by punching a series of eight IBM cards, each of which was prefaced by a code indicating the run number and running conditions. These cards were later analyzed by an IBM 709 computer, by using a program described in Sec. IV.

III. EXPERIMENTAL PROCEDURE

We took data at the three laboratory angles of 6.2, 32.0, and 60.5 deg. At each angle data were taken with hydrogen in the target, with deuterium, and with the target empty. Target in-out ratios of approximately 5:1 were obtained with hydrogen, and 12:1 with deuterium. The deuterium data will be analyzed separately and are not reported here.

Both the 180-deg and the circular spectrometer were used at all angles. With each spectrometer we took data at each of 16 magnetic field settings, ranging from 1.92 to 19.7 kG, each field setting differing from the previous one by a factor of 1.168. The purpose of running at so many different fields was to average out the effect of possible small variations in efficiencies of individual counters or counter combination. Discontinuities in the observed spectrum due to systematic variations in counter efficiencies are essentially eliminated if the value at each experimental point is determined by contributions from almost every possible combination of counters.

A run under a given set of conditions typically lasted about 15 minutes, after which we turned off the counters in order to read out the data. Time was allocated to converter-in and converter-out operations approximately in proportion to the

square roots of the counting rates, in order to minimize the statistical error for a fixed amount of running time. The observed converter in-out ratio varied between 1.5:1 and 15:1, depending on the experimental conditions.

IV. DATA ANALYSIS AND CORRECTIONS

As previously mentioned, our experimental method differed from that of other workers in the field of pair spectrometry in one important respect: rather than take data at only one, or at most a few magnetic field settings, we varied our magnetic field in small increments over a very wide range. This posed a rather unusual problem in the data analysis. At each field setting, as many as 36 different energy channels (with the circular spectrometer) are defined, depending upon the particular combination of counters producing the coincidence. Since we collected data at 16 different magnetic fields, this meant that there were 576 different energy channels between minimum and maximum energy.

Conventional pair spectrometers have certain symmetry properties which greatly reduce this number. However, with the circular geometry shown in Fig. 3 all these symmetry properties were destroyed. Conceptually the data analysis was no more difficult but the amount of labor involved was now enormously greater. For this reason it was imperative to use a high speed computer to analyze the data. A program was written for the IBM 709 which: (a) divided the gamma-ray spectrum into energy increments, (b) placed the events from each energy channel of the pair spectrometer into its appropriate energy increment, (d) applied the corrections that had been previously calculated by other computer programs (d) performed the target in-out and converter in-out subtractions, and (e) calculated the errors.

The data were corrected for the following effects:

a. Variation of spectrometer geometric efficiency with magnetic field
b. Variation of pair-production cross section vs energy
c. Loss of events due to vertical scattering by the converter of electrons and positrons out of the plane of the scintillators
d. Radiation straggling of electrons and positrons in the converter.

Regarding the first effect, it is easy to show that the geometric efficiency of a pair spectrometer is proportional to the magnetic field. For the pair-production cross section we used the theory given by Bethe and Heitler,[18] as summarized by Bethe and Askin[19] and modified by Davies et al.,[20] to account for deviations from the Born approximation. To calculate the vertical scattering, we used the plural scattering theory of Molière.[21] For the radiation-straggling correction we again made use of the calculations of Bethe and Heitler.[18] These corrections were all calculated by means of IBM 709 computer programs.

A thorough discussion of these corrections will be given in the article describing the pair spectrometers, to which previous reference has been made.[16] Figure 5 shows the spectra obtained at 650 deg—after all corrections have been made—with the circular spectrometer and the 180-deg spectrometer, plotted separately. A few percent adjustment of the normalization of one spectrometer to the other has been made. The close similarity in the spectral shapes obtained with two spectrometers of such widely differing geometries gave us considerable confidence in the analysis described above.

V. RESULTS

The gamma-ray spectra observed at the three lab angles of 6, 32, and 60 deg are shown in Fig. 6. The high-energy cutoffs predicted by π^0 decay kinematics are at 540, 464, and 346 MeV, respectively. In each case the experimental cutoffs are almost exactly where predicted. Kinematics predict a low-energy cutoff as well, at energies of 27, 23, and 17 MeV, respectively. Although the spectra did drop off sharply at the low-energy end, they never actually reached zero. This was probably due to multiple radiation processes in the collimators by which a high-energy gamma ray can produce one or more low-energy gamma rays.

The errors shown are statistical errors only. The errors on most points are less than 2% except at the lowest energies. In addition, there are systematic

errors of as much as 5%, which would affect the total normalization of the spectra. These errors come primarily from uncertainties in the measurement of the proton current, due to problems encountered with the secondary-emission monitor chamber.

In Fig. 7 we show the same gamma-ray spectra after they have been transformed into the two-proton barycentric system. In this system the predicted high-energy cutoffs are now all at the same energy: 301 MeV. The predicted low-energy cutoff is 15 MeV.

The errors shown in Fig. 7 are larger than those shown in Fig. 6. This is because a reproducibility error, estimated to be equal to 2% of the value of each point, has been added to the statistical error. This was done in order to make the goodness-of-fit parameter $\chi^2/d = 1$ in the least-squares analysis to be described below. The χ^2 is the total squared deviation and d is the number of degrees of freedom.

VI. ANALYSIS

Because there is no analytic way to deduce neutral-pion spectra from gamma-ray spectra, a pion spectrum was fit to the data by trial and error by using the method of least squares. A computer program was written which computed the gamma-ray spectrum due to an assumed pion spectrum. This spectrum contained three angular terms—isotropic, $\cos^2\theta$, and $\cos^4\theta$—and momentum terms that were given by the three-body final-state phase space multiplied by a power series in the barycentric pion momentum. This power series contained terms up to and including the eighth power. That is, the pion spectrum was assumed to be of the form

$$\frac{d\sigma_{\pi^0}}{dp d\Omega} = f(p)\left[\sum_0^8 a_n p^n + \left(\sum_0^8 b_n p^n\right)\cos^2\theta + \left(\sum_0^8 c_n p^n\right)\cos^4\theta\right], \qquad (3)$$

where $f(p)$ is equal to three-body final-state phase space.

The parameters a_n, b_n, c_n were all varied until χ^2 between the gamma-ray spectrum predicted by (3) and the data were minimized.

The curves in Fig. 7 show the gamma-ray spectra resulting from (3) with the best values of the parameters determined by the least-squares analysis. The excellent fit obtained is the basis for our statement that there is no evidence for high-energy gamma rays produced by any source other than neutral-pion decay.

Because of the unreliability of the data at the low-energy end of the spectrum, as discussed in Sec. V, they were not included in the least-squares analysis. They comprise the points below 55 MeV in Fig. 7, as indicated by the dashed line. The results of the least-squares analysis were insensitive to the exact value of this cutoff energy.

The corresponding pion momentum spectra at 0, 45, and 90 deg in the barycentric system are shown in Fig. 8. The dotted curve represents the pion spectrum given by phase space, assuming an isotropic angular distribution. The curves in Fig. 8 are normalized to our observed total cross section

$$\sigma_T = 3.46 \pm 0.25 \text{ mb}, \tag{4}$$

which is included in the plot of Fig. 1. We obtained (4) by integrating (3) over angle and energy, using the best values for the parameters. The error is due primarily to the uncertainty in the measurement of the absolute proton flux striking the hydrogen target.

The angular distribution of pions for the spectra plotted in Fig. 8 is represented by

$$\frac{d\sigma_{\pi^0}}{d\Omega} = \frac{\sigma_T}{4\pi}\left[0.834 + 0.099(3\cos^2\theta) + 0.067(5\cos^4\theta)\right]. \tag{5}$$

A fit that was almost as good was obtained by using only the isotropic and $\cos^2\theta$ terms in (3). For this fit the angular distribution is given by

$$\frac{d\sigma_{\pi^0}}{d\Omega} = \frac{\sigma_T}{4\pi}\left[0.79 + 0.21(3\cos^2\theta)\right]. \tag{6}$$

The momentum spectra, however, were virtually the same as those plotted in Fig. 8. Note that the fraction of π^0's emitted isotropically in solution (6) is about the same as that in solution (5), namely about 80%.

VII. CONCLUSIONS

We now may compare our pion angular distributions with those of Dunaitsev and Prokoshkin.[5] They assumed that the pion angular distribution was given by

$$\frac{d\sigma_{\pi^0}}{d\Omega} \propto \frac{1}{3} + b\cos^2\theta, \tag{7}$$

and used their measurements to determine the value of the parameter b from 500 to 665 MeV. They find b to be statistically zero except at 665 MeV where $b = 0.10 \pm 0.03$. Their results are shown in Fig. 9. In order to make a direct comparison with our results, we used the solution given by Eq. (6), in which the $\cos^4\theta$ term was omitted. From Eq. (6), $b = 0.27 \pm 0.04$. The error was estimated by noting the approximate sensitivity of χ^2 to b. Our value for b at 735 MeV is also plotted in Fig. 9. It appears from this figure that b, though still small, is rising rapidly above 600 MeV.

It is perhaps somewhat surprising that the pion angular distribution is so nearly isotropic. Most nuclear processes become quite anisotropic as energy increases. At the energy at which this experiment was performed, partial waves through $\ell = 2$ should be important. However, if the production proceeds primarily through the intermediate creation of a nuclear isobar, which subsequently decays into a proton and a π^0 meson, one expects the reaction to be nearly isotropic. After creation of the isobar, very little kinetic energy remains. In our case, approximately 40 MeV is available to the proton and an isobar of mass 1230 MeV. The isobar would therefore be produced primarily in an s state. The angular distribution of the pions would then be nearly isotropic if we assume that the isobars are not polarized.[22] The presence of small $\cos^2\theta$ and $\cos^4\theta$ terms indicates that either there is some p- and perhaps d-wave production of the isobar, or that not all production proceeds

through creation of an isobar.

In Fig. 10 we compare our results to the isobar-model calculation of Lindenbaum and Sternheimer.[23] The solid curve represents the pion momentum spectrum deduced from our experiment and integrated over solid angle. That is

$$\frac{d\sigma_{\pi^0}}{d\eta} = \int \frac{d^2\sigma_{\pi^0}}{d\eta d\Omega} \, d\Omega, \tag{8}$$

where $\eta = p/\mu c$.

The curve labeled "isobar model" represents the pion momentum spectrum calculated by Lindenbaum and Sternheimer at 800-M lab proton energy. In this calculation they assumed isotropic isobar production and decay. All momenta on the abscissa for this curve have been adjusted in order to make the maximum allowable momentum the same as that at our energy of 735 MeV.

We feel that the comparison is still valid even though the energy at which Lindenbaum and Sternheimer made their calculation was 800 MeV, and that at which our data was taken was 735 MeV. This is because the difference in available energy in the barycentric system is only 27 MeV at the above two lab energies whereas the width of the isobar resonance is about 140 MeV.

The curve labeled "phase space" represents the three-body final-state phase space, assuming isotropic pion production. All three curves in Fig. 10 have been normalized to the total cross section given by Eq. (4).

There is some disagreement between the detailed shapes of the pion spectra given by experiment and the isobar model. (The discrepancy for $\eta < 1$ could be due to multiple π^0 production which we have ignored.[9]) Nevertheless, it is clear that the isobar model gives much better agreement than does a phase space distribution. In particular, there is a strong enhancement of pion production in the region $\eta = 1.5$ to 1.7, shown by both experiment and the isobar-model calculation, which is not as pronounced in the phase space distribution.

On the basis of this comparison in Fig. 10 we conclude that at 735-MeV lab proton energy the isobar model mechanism is prominent in reaction (1).

VIII. ACKNOWLEDGMENTS

First, we would like to thank Mr. Paul McManigal who helped us during most of our runs and who contributed many valuable ideas to this experiment. Also, we would like to thank Mr. Donald Hagge for the generous assistance he gave us during the running of the experiment.

FOOTNOTE AND REFERENCES

*Work done under the auspices of the U. S. Atomic Energy Commission.

1. J. W. Mather and E. A. Martinelli, Phys. Rev. 92, 780 (1953).
2. W. E. Crandall and B. J. Moyer, Phys. Rev. 92, 749 (1953); W. E. Crandall, Ph. D. Thesis, University of California Radiation Laboratory Report UCRL-1637, 1952 (unpublished).
3. M. Gell-Mann and K. H. Watson, Ann. Rev. Nuclear Sci. 4, 219 (1954).
4. A. H. Rosenfeld, Phys. Rev. 96, 139 (1954).
5. A. F. Dunaitsev and Iu D. Prokoshkin, Soviet Phys. JETP (English Transl.) 9, 1179 (1959).
6. R. A. Stallwood, R. B. Sutton, T. H. Fields, J. G. Fox, and J. A. Kane, Phys. Rev. 109, 1716 (1958); R. A. Stallwood, Ph. D. Thesis, Carnegie Institute of Technology Report NYO-7108, March 1956 (unpublished).
7. J. Marshall, L. Marshall, V. A. Nedzel, and S. D. Warshaw, Phys. Rev. 88, 632 (1952).
8. I. S. Hughes, P. V. March, H. Muirhead, and W. O. Lock, Phil. Mag., Ser. 8, 2, 215 (1957).
9. A. P. Batson, B. B. Culwick, J. G. Hill, and L. Riddiford, Proc. Roy. Soc. (London), Ser. A, 251, 218 (1959).
10. B. J. Moyer and R. K. Squire, Phys. Rev. 107, 283 (1957).
11. Iu. D. Prokoshkin and A. A. Tiapkin, Soviet Phys. JETP (English Transl.) 5, 618 (1957).
12. C. York, R. March, W. Kernan, and J. Fischer, Phys. Rev. 113, 1339 (1959).
13. Iu. D. Baiukov and A. A. Tiapkin, Soviet Phys. JETP (English Transl.) 5, 779 (1957).

14. This experiment is reported in greater detail by Gilbert D. Mead, Ph. D. Thesis, Lawrence Radiation Laboratory Report UCRL-10187, May 1962 (unpublished).

15. R. Larsen, Experiments on Neutron-Proton Scattering and Determination of the Pion-Nucleon Coupling Constant, Ph. D. Thesis, Lawrence Radiation Laboratory Report UCRL-9292, July 1960 (unpublished).

16. G. D. Mead, R. J. Conce, and D. L. Lind, Lawrence Radiation Laboratory Report UCRL-10781, April 1963, Rev. Sci. Instr. (to be submitted).

17. W. Wenzel, Millimicrosecond Coincidence Circuit for High-Speed Counting, University of California Radiation Laboratory Report UCRL-8000, October 1957 (unpublished).

18. H. A. Bethe and W. Heitler, Proc. Roy. Soc. (London), Ser. A, 146, 83 (1934).

19. H. A. Bethe and J. Ashkin, Passage of Radiations through Matter, in Experimental Nuclear Physics, Vol. I., ed. by E. Segrè (John Wiley and Sons, Inc., New York, 1953).

20. H. Davies, H. A. Bethe, and L. C. Maximon, Phys. Rev. 93, 788 (1954).

21. G. Moliere, Z. Naturforsch., 3a, 78 (1948).

22. See footnote 19, in reference 23.

23. S. J. Lindenbaum and R. M. Sternheimer, Phys. Rev. 105, 1874 (1957).

FIGURE CAPTIONS

1. Total cross section for the reaction $p + p \rightarrow p + p + \pi^0$. η_{max} is the maximum pion momentum in the barycentric system, in units of $m_\pi c$.
2. Experimental layout at $\theta_{lab} = 6$ deg. M_1 and M_2 guide the proton beam, M_3 and M_4 act as sweeping magnets, and M_5 is the spectrometer magnet.
3. The circular spectrometer.
4. Block diagram of the electronics.
5. Spectra obtained with the circular spectrometer and the 180-deg spectrometer, plotted separately.
6. Gamma-ray energy spectra as measured in the laboratory.
7. The gamma-ray spectra after transformation into the barycentric system. All quantities in this figure have been transformed into the barycentric system. The curves represent the gamma-ray spectra resulting from the neutral-pion spectra giving the best fit to the data as determined by the least-squares analysis. Data to the left of the vertical dashed line were not included in this analysis.
8. The neutral-pion spectra in the barycentric system which give the gamma-ray spectra plotted in Fig. 6. The dotted curve represents the pion spectrum given by the three-body final-state phase space. It is normalized to give the same total cross section as the solid curves, assuming an isotropic angular distribution.
9. Values of the coefficient b in the expansion

$$\frac{d\sigma_{\pi^0}}{d\Omega} \propto \frac{1}{3} + b\cos^2\theta.$$

10. Pion momentum spectra in the barycentric system.

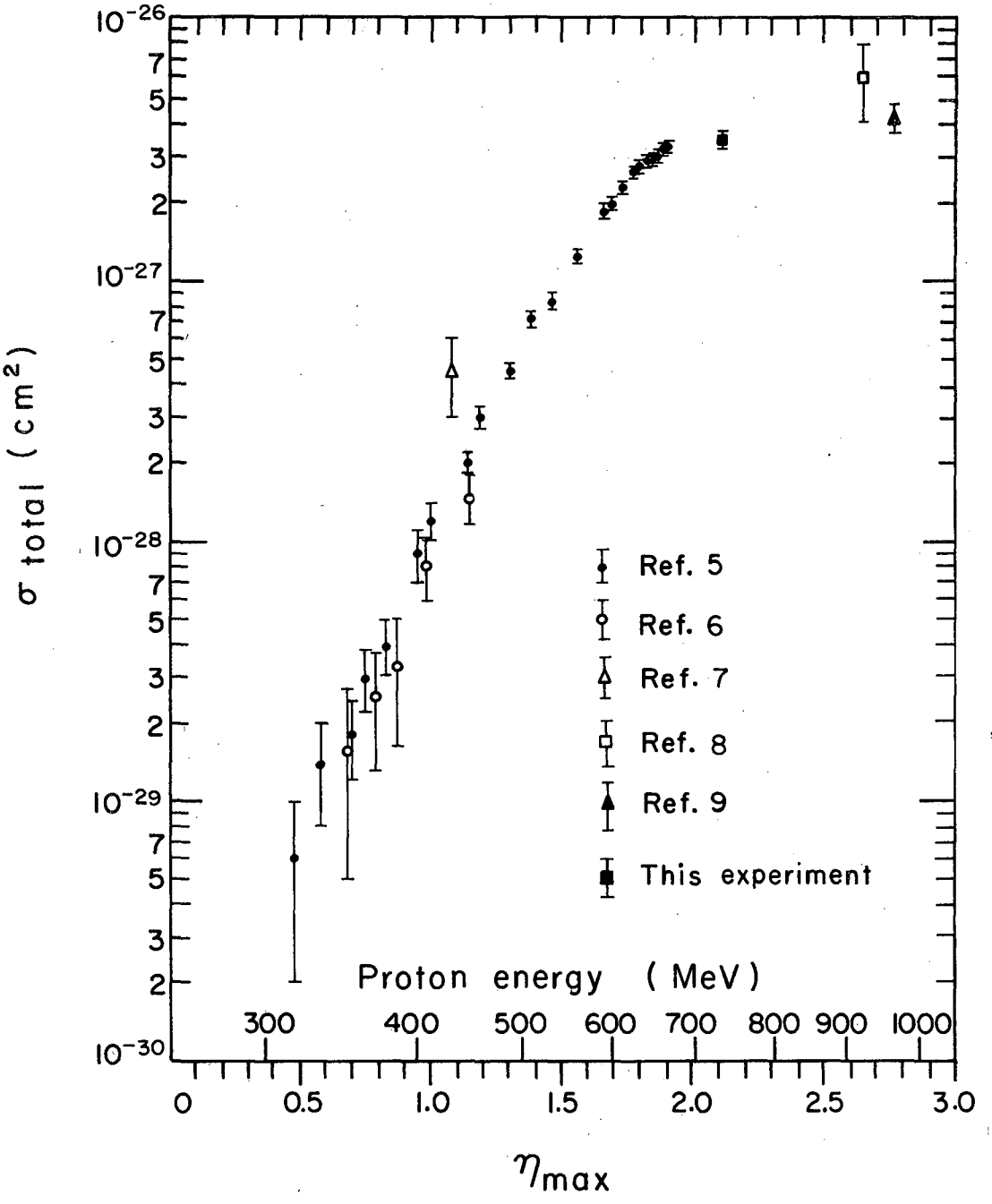
σ total (cm²)
10⁻²⁶
10⁻²⁷
10⁻²⁸
10⁻²⁹
10⁻³⁰
Ref. 5
Ref. 6
Ref. 7
Ref. 8
Ref. 9
This experiment
Proton energy (MeV)
300
400
500
600
700
800
900
1000
0
0.5
1.0
1.5
2.0
2.5
3.0
ηmax
MUB-1083

Fig. 1

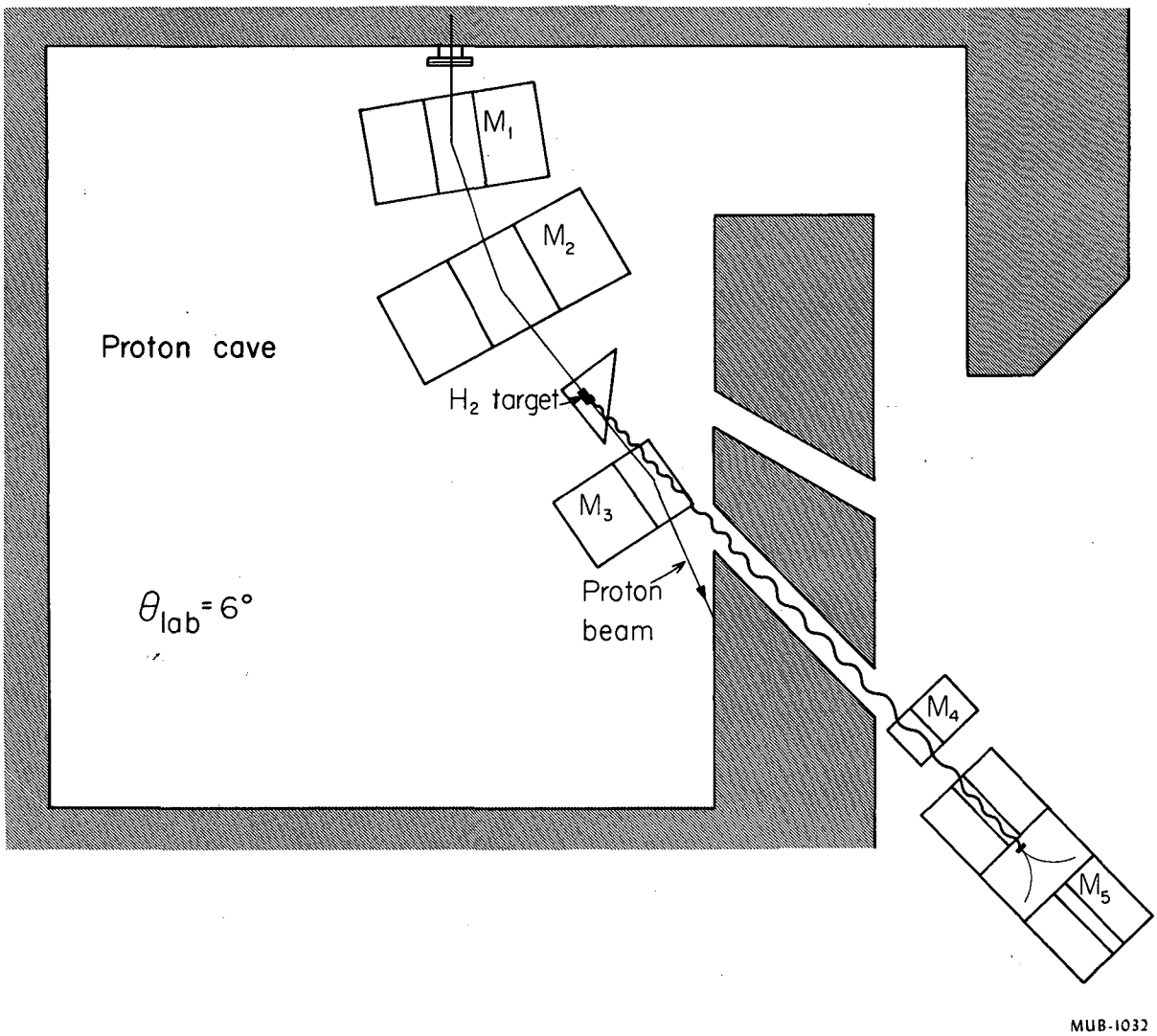
M1
M2
Proton cave
H2 target
M3
θlab = 6°
Proton
beam
M4
M5
MUB-1032

Fig. 2

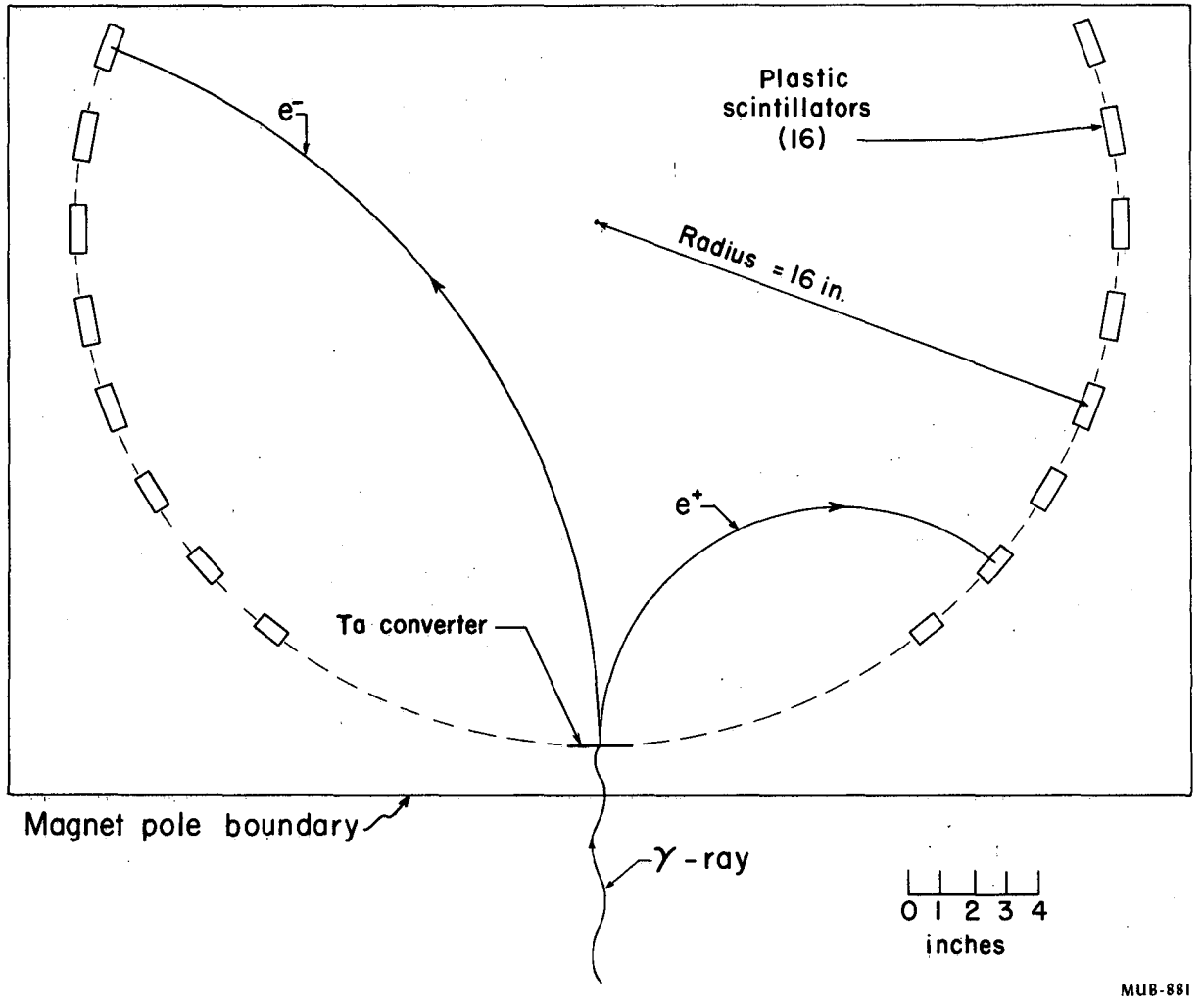
Plastic
scintillators
(16)
e⁻
Radius = 16 in.
e⁺
Ta converter
Magnet pole boundary
γ-ray
0 1 2 3 4
inches
MUB-881

Fig. 3

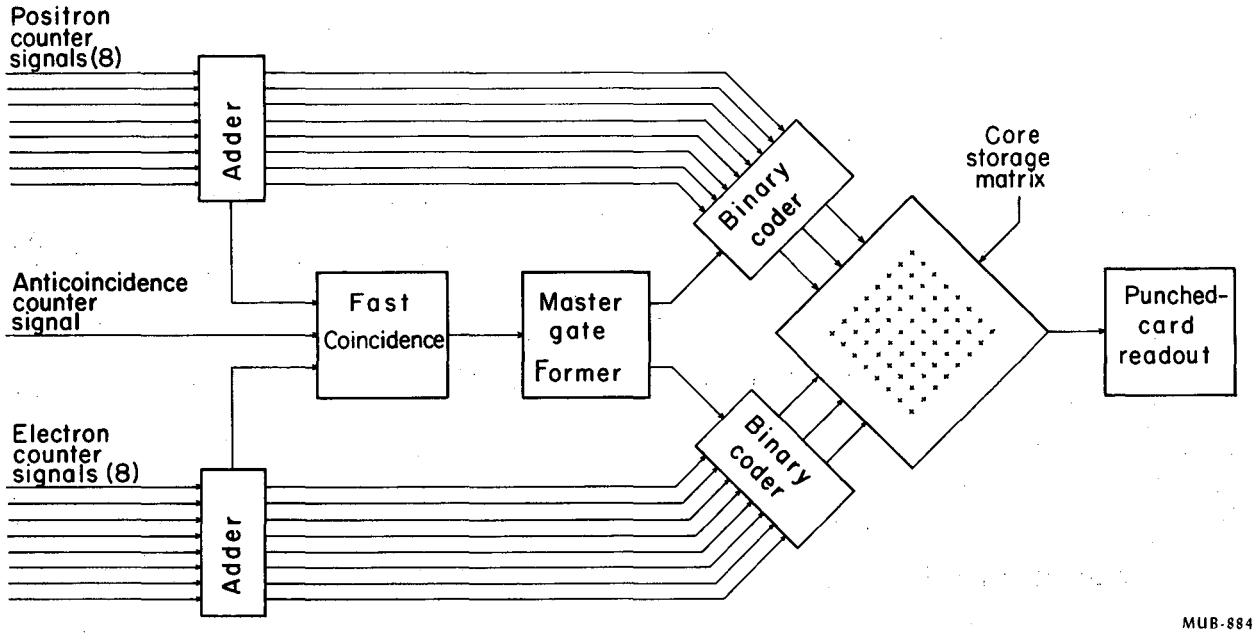
Positron counter signals (8)
Adder
Anticoincidence counter signal
Fast Coincidence
Master gate Former
Electron counter signals (8)
Adder
Binary coder
Binary coder
Core storage matrix
Punched-card readout
MUB-884

Fig. 4

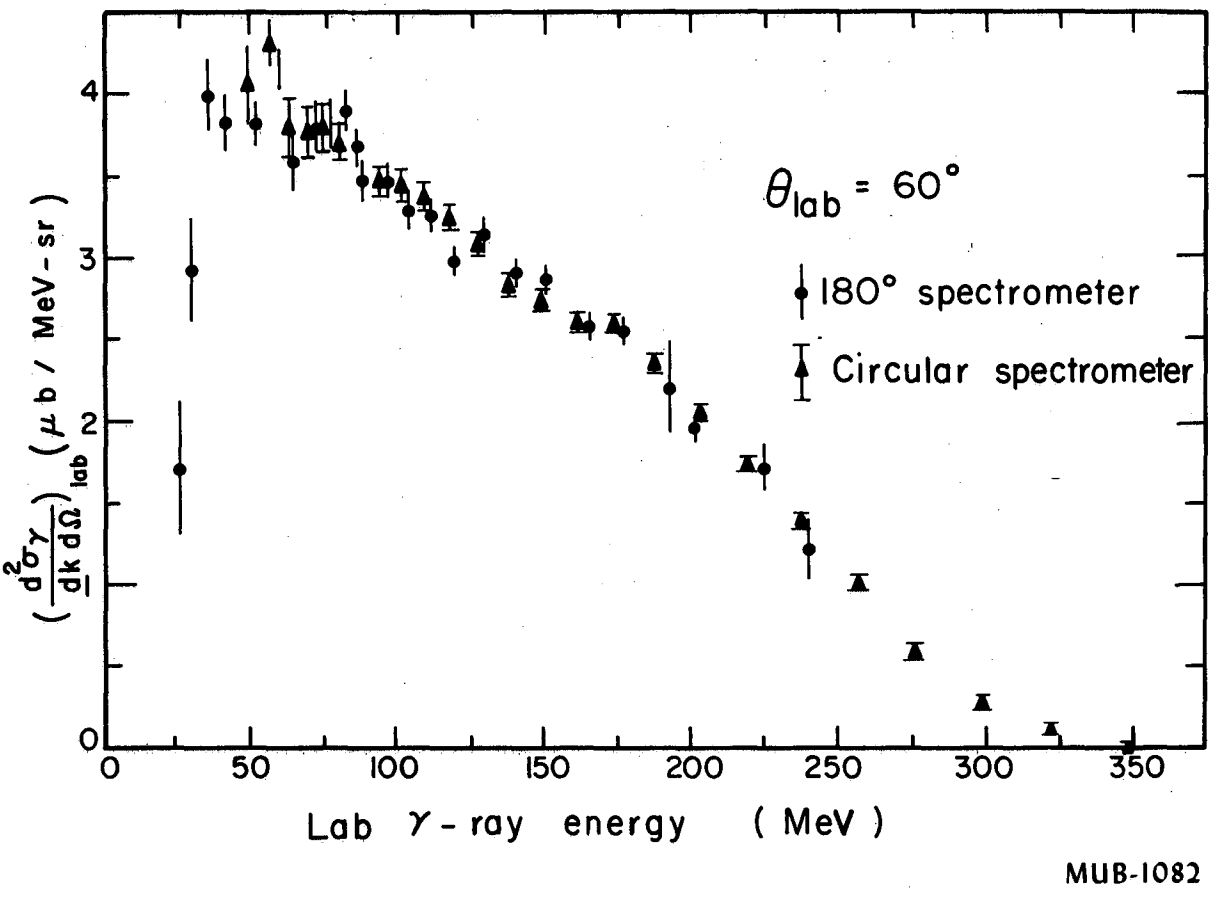
θ_{lab} = 60°
180° spectrometer
Circular spectrometer
$(\frac{d^2\sigma_\gamma}{dk\,d\Omega})_{lab}$ (μb / MeV-sr)
Lab γ-ray energy (MeV)
0
50
100
150
200
250
300
350
1
2
3
4
MUB-1082

Fig. 5

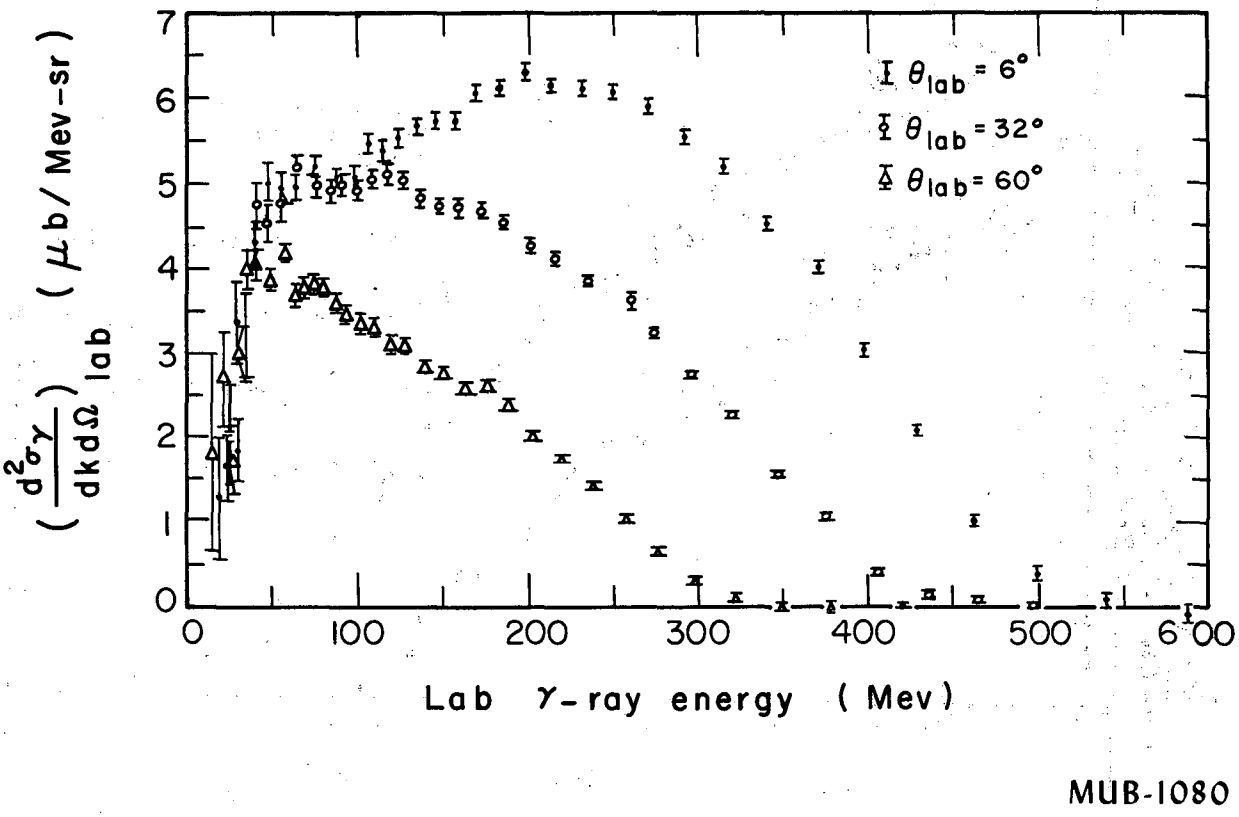
$\left(\frac{d^2\sigma_\gamma}{dk\,d\Omega}\right)_{lab}$ (μb / Mev-sr)
θ_{lab} = 6°
θ_{lab} = 32°
θ_{lab} = 60°
0
1
2
3
4
5
6
7
0
100
200
300
400
500
600
Lab γ-ray energy (Mev)
MUB-1080

Fig. 6

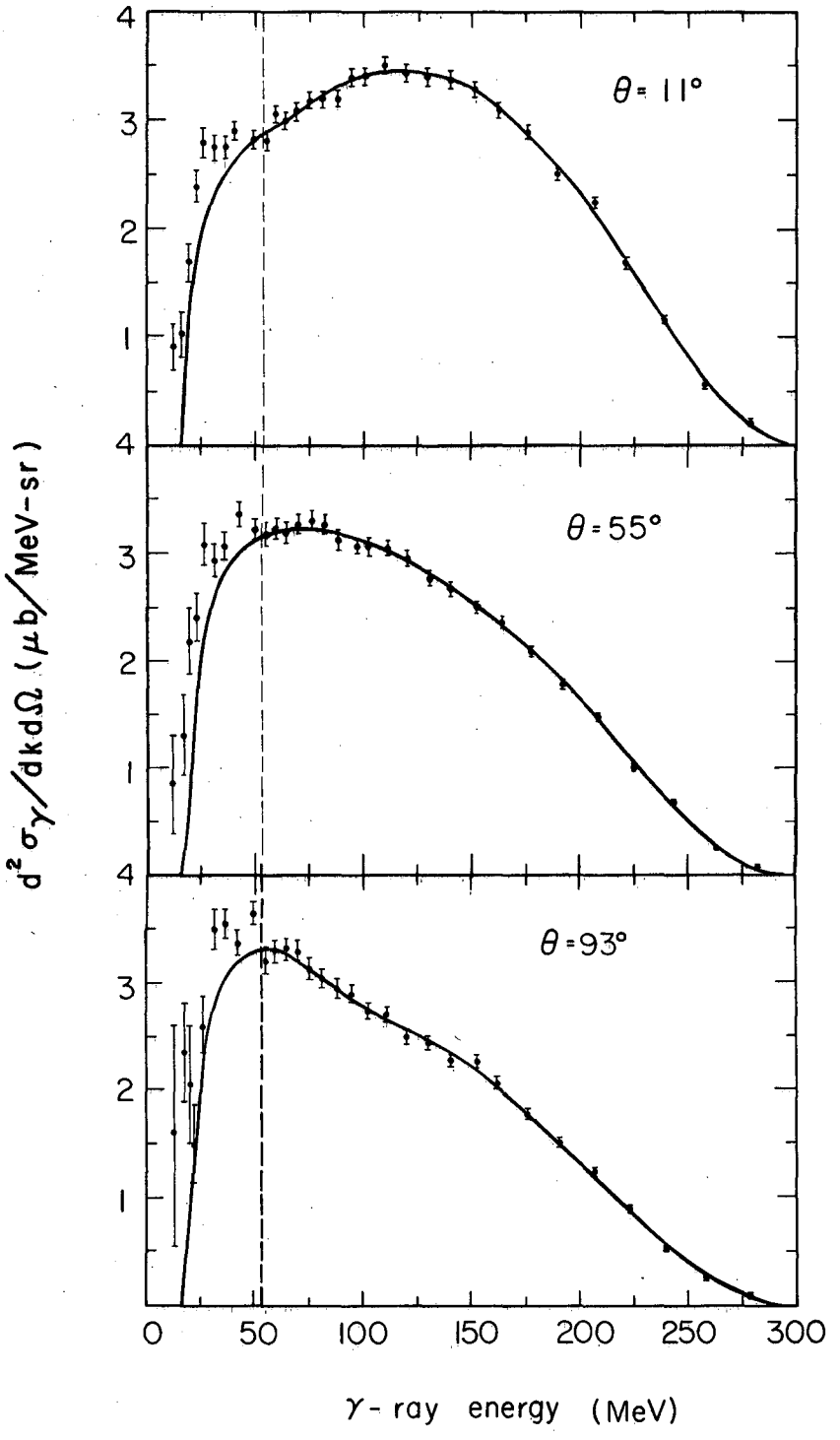
θ = 11°
θ = 55°
θ = 93°
$d^2\sigma_\gamma/dkd\Omega$ (μb/MeV-sr)
γ - ray energy (MeV)
0
50
100
150
200
250
300
1
2
3
4
MUB-1359

Fig. 7

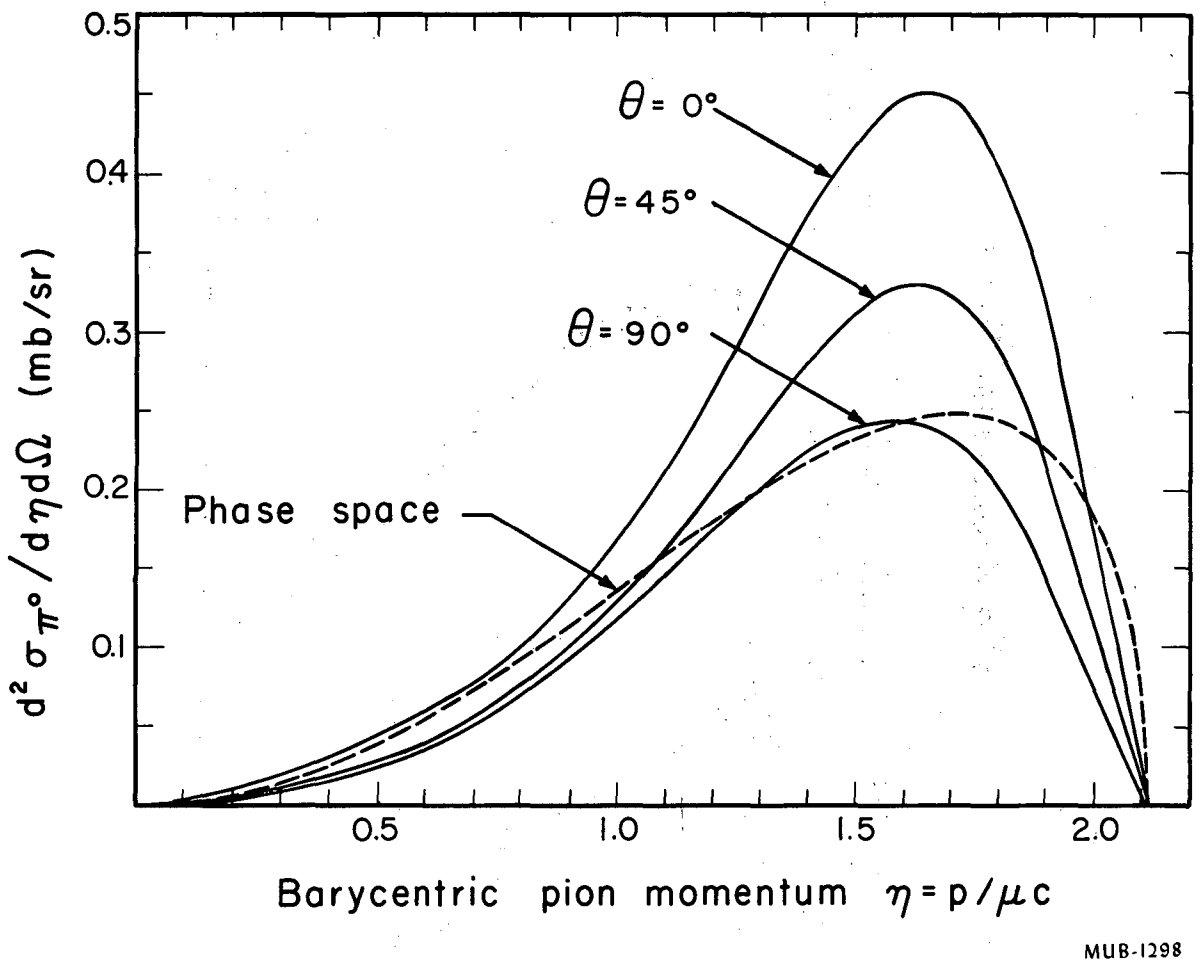
0.5
0.4
0.3
0.2
0.1
$d^2\sigma_{\pi^0}/d\eta d\Omega$ (mb/sr)
$\theta = 0°$
$\theta = 45°$
$\theta = 90°$
Phase space
0.5
1.0
1.5
2.0
Barycentric pion momentum $\eta = p/\mu c$
MUB-1298

Fig. 8

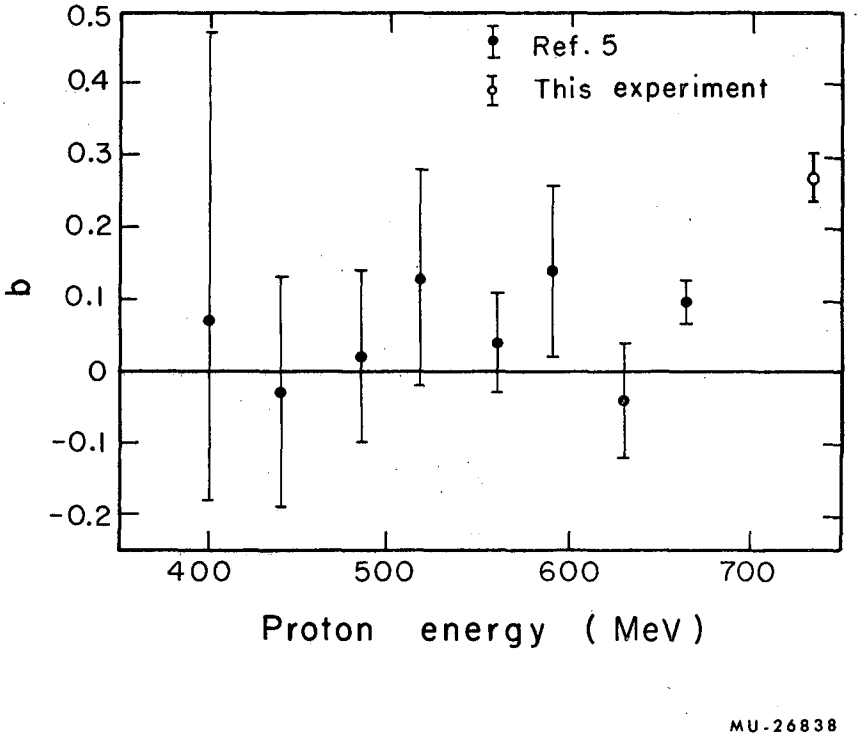
0.5
0.4
0.3
0.2
0.1
0
-0.1
-0.2
b
Ref. 5
This experiment
400
500
600
700
Proton energy (MeV)
MU-26838

Fig. 9

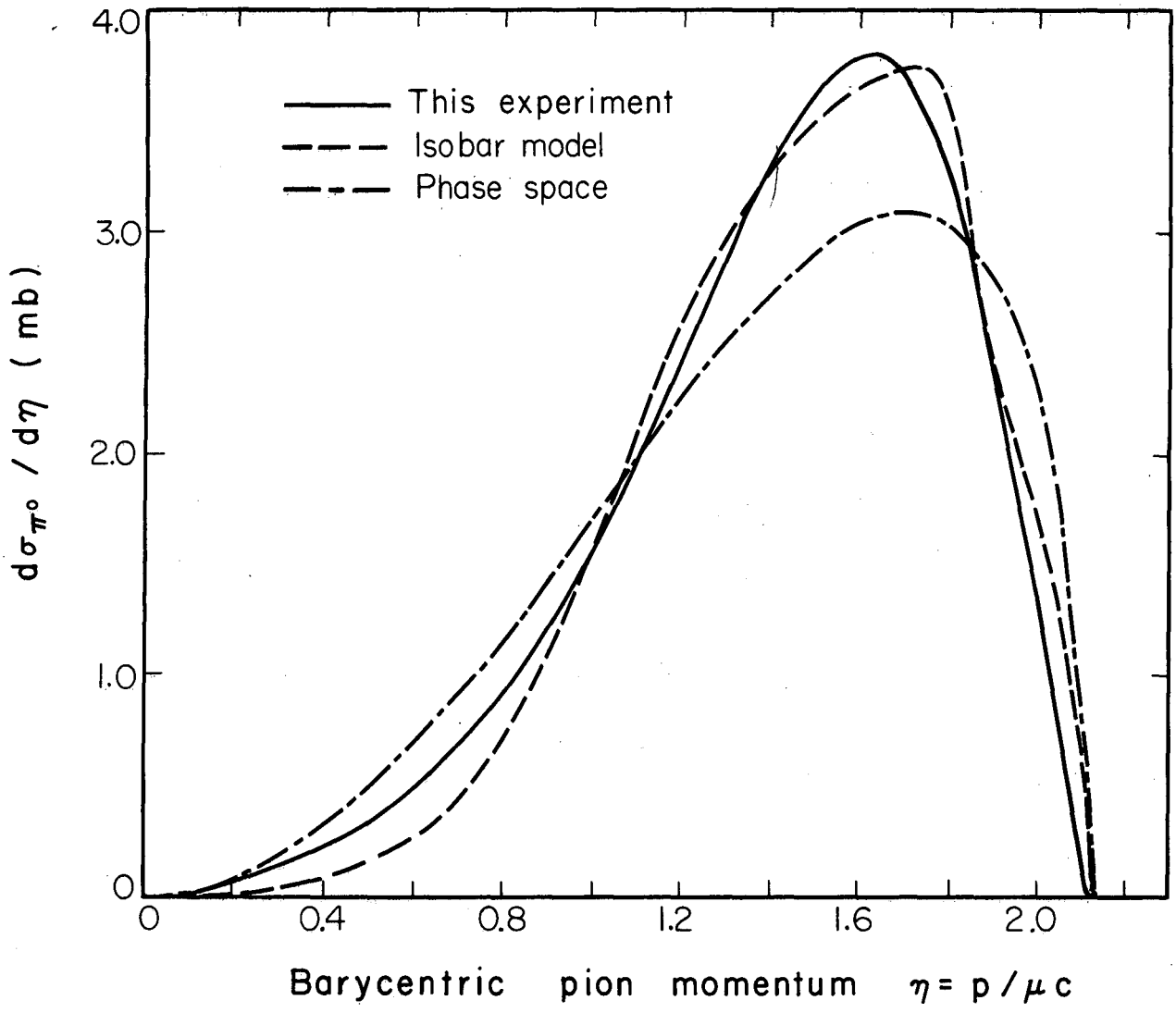
4.0
3.0
2.0
1.0
0
0
0.4
0.8
1.2
1.6
2.0
This experiment
Isobar model
Phase space
$d\sigma_{\pi^0} / d\eta$ (mb)
Barycentric pion momentum $\eta = p / \mu c$
MUB-1383

Fig. 10